Application of the correlation coefficient method for determination of the focal plane to digital particle holography

Yan Yang,[1,2] Bo-seon Kang,[2,*] and Yeon-jun Choo[3]

[1]Department of Mechanic, Chongqing Institute of Technology, Chongqing 400050, China
[2]Department of Mechanical Engineering, Chonnam National University, Gwangju 500-757, South Korea
[3]Thermal Hydraulics Safety Research Center, Korea Atomic Energy Research Institute, Taejon 305–600, South Korea

*Corresponding author: bskang@chonnam.ac.kr

Received 14 August 2007; revised 11 December 2007; accepted 11 December 2007;
posted 14 December 2007 (Doc. ID 86488); published 19 February 2008

The correlation coefficient (CC) method, which was proposed by our research group, is applied to digital particle holography to locate the focal plane of particles. It uses the fact that the CC is maximum at the focal plane. The factors influencing this method are discussed with a numerical simulation of holograms. For real holograms, the Wiener filter was proposed to process both recorded holograms and reconstructed images. The application results using the dot array target showed that the Wiener filter is a very effective tool for processing holography-related images. The effects of the dot size and the object distance on the errors in the determination of the focal plane by the CC method were investigated by using the calibration target. © 2008 Optical Society of America

OCIS codes: 090.0090, 090.1995.

1. Introduction

Holography is an effective tool in various scientific and engineering fields with a wide range of applications. It is a 3D imaging process, which can instantaneously capture the volumetric information of measurement fields. With the rapid development of CCD cameras and computers, digital holography was explored. It does not need a chemical process such as optical holography and has several strengths such as high efficiency, simplicity, and the ability for real time analysis. Therefore, it can be used in many practical measurement fields [1].

Digital particle holography is a promising tool for analyzing particle features such as size, velocity, and spatial distributions. One of the main problems, however, is how to find the location of the best focal plane of particles along the optical axis. Various methods have been suggested to determine the focal plane. Yu and Cai investigated a criterion based on gradient computation [2], Dubois *et al.* introduced a method that uses the score of the integrated amplitude modulus [3], Lefebvre *et al.* showed that the maximum modulus of wavelet transform was reached at the best focal plane [4], and Zhang *et al.* located the focal plane by using the Gabor transform [5].

The correlation coefficient (CC) method was first presented by Choo and Kang [6] in our research group to determine the focal plane of particles in optical holography. This method in optical holography, however, can only be used for locating the focal plane of large particles ($D_d > 50$ μm). In this paper, the CC method is applied to digital holography to determine the focal plane of various size particles, including much smaller size particles ($D_d \sim 10$ μm). Using a numerical simulation of holograms, the factors influencing this method were discussed, and the optimal values of the parameters involved in this method were obtained. For real holograms obtained by experimental recording, the Wiener filter was first proposed to process recorded holograms and reconstructed images. Finally, the effects of the dot size and the object distance on the errors in the determination of the focal plane by the CC method were investigated by using the calibration target.

0003-6935/08/060817-08$15.00/0
© 2008 Optical Society of America

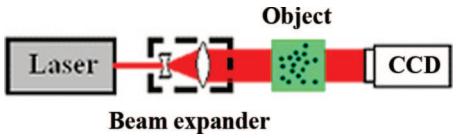

Fig. 1. (Color online) Optical setup of in-line digital holography.

2. Focusing Method

A. Principle of In-Line Digital Holography

Digital holography is classified as in line or off axis depending on the optical setup. In-line digital holography, shown in Fig. 1, is widely used because it has a simple optical configuration. A laser beam is expanded by an expander and goes through the object field. The part of the beam diffracted by objects is considered to be the object beam, and the one coming without distortion onto the recording surface (a CCD camera) is considered to be the reference beam. The superposition of the two beams creates an interference pattern (in-line hologram) on a CCD camera.

The reconstruction equation of an in-line digital hologram can be described by the Fresnel–Kirchhoff integral [7]

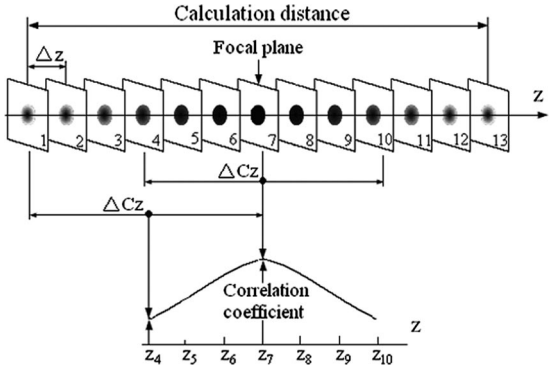

Fig. 3. CC method.

The coordinates of Eqs. (1) and (2) are shown in Fig. 2. $R(\xi', \eta')$, $h(x, y)$, and $E_R(x, y)$ are functions of the reconstruction image, hologram, and reference, respectively; d is the distance between two adjacent planes, λ is the wavelength, and ρ is the distance between two corresponding points in two adjacent planes.

The Fresnel approximation or the convolution approach can be used for numerical reconstruction of Eq. (1). The reconstruction equation by the convolution approach, which is used in this study, can be expressed as [7]

$$R(\xi', \eta') = F^{-1}\left\{F[h(x, y)]F\left[\frac{i}{\lambda}\frac{\exp\left[-i\frac{2\pi}{\lambda}\sqrt{\left(d^2+\left(x-\frac{N}{2}\right)^2\Delta x^2+\left(y-\frac{N}{2}\right)^2\Delta y^2\right)}\right]}{\sqrt{\left(d^2+\left(x-\frac{N}{2}\right)^2\Delta x^2+\left(y-\frac{N}{2}\right)^2\Delta y^2\right)}}\right]\right\}, \tag{3}$$

$$R(\xi', \eta') = \frac{i}{\lambda}\int_{-\infty}^{\infty}\int_{-\infty}^{\infty} h(x, y)E_R(x, y) \times \frac{\exp\left(-i\frac{2\pi}{\lambda}\rho\right)}{\rho}\,dxdy, \tag{1}$$

with

$$\rho = \sqrt{(\xi' - x)^2 + (\eta' - y)^2 + d^2}. \tag{2}$$

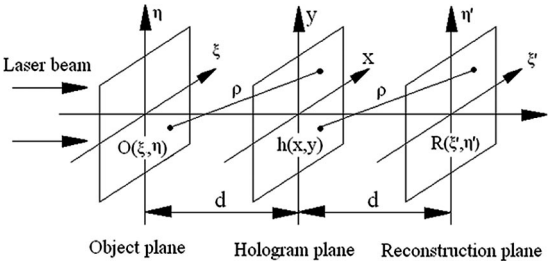

Fig. 2. Coordinate system.

where N is the pixel number, Δx and Δy are the resolutions of the hologram, and $F[\,]$ and $F^{-1}[\,]$ are Fourier transform and inverse Fourier transform, respectively. The intensity of the reconstruction image is calculated by

$$I = |R(\xi', \eta')|^2. \tag{4}$$

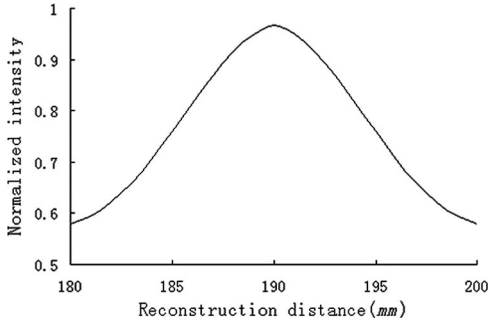

Fig. 4. Typical curve shape of intensity distribution of reconstruction images with particle size, D_d = 300 μm and object distance, d = 190 mm.

The numerical simulation of holograms that has no noise and other influencing factors can be a successful solution for verifying various holographic criteria. It is based on the fact that the procedure for a reconstruction image from a hologram is identical to that for the generation of a hologram from an object image in Fig. 2. After changing some variables in Eq. (1), we can obtain the hologram function

$$h(x, y) = \frac{i}{\lambda}\int_{-\infty}^{\infty}\int_{-\infty}^{\infty} O(\xi, \eta)E_R(\xi, \eta) \times \frac{\exp\left(-i\,\frac{2\pi}{\lambda}\,\rho\right)}{\rho}\,d\xi d\eta, \quad (5)$$

with

$$\rho = \sqrt{(x-\xi)^2 + (y-\eta)^2 + d^2}, \quad (6)$$

where $O(\xi, \eta)$ is an object function. Because the form of Eq. (5) is the same as that of Eq. (1), the convolution approach can also be used to obtain the simulation hologram from the object image [8].

According to the object distance, holography is also classified as Fresnel (near field) or Fraunhofer (far field) holography. In this paper, Fresnel holography is investigated, and the minimum object distance in Fresnel holography is presented by [9]

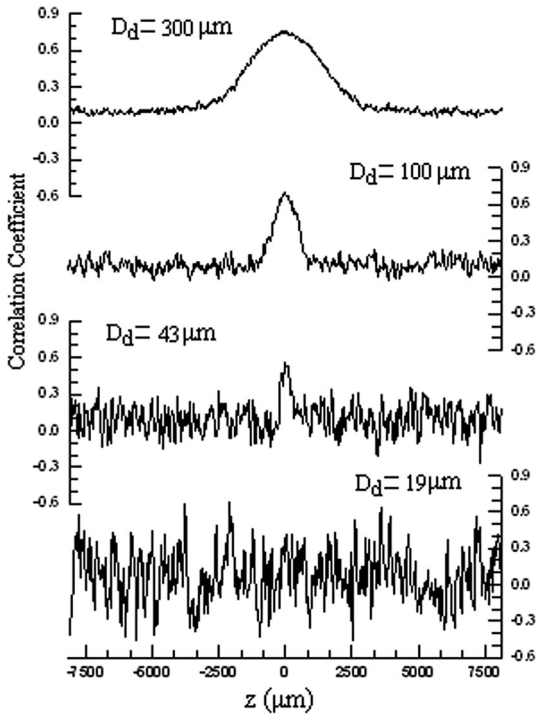

Fig. 5. CC method applied to different size particles in optical holography (from [6]).

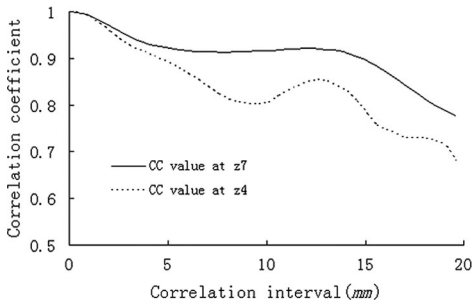

Fig. 6. CCs by different correlation intervals (object distance, d = 150 mm).

$$d \geq \sqrt[3]{\frac{1}{8}\,\frac{\left[(\xi-x)^2 + (\eta-y)^2\right]^2}{\lambda}} = \sqrt[3]{\frac{1}{8}\,\frac{\left[N^2(\Delta\xi-\Delta x)^2 + N^2(\Delta\eta-\Delta y)^2\right]^2}{\lambda}}, \quad (7)$$

where $\Delta\xi$ and $\Delta\eta$ are the resolutions of the object image. In this paper, N is 2048, λ is 0.6328 μm, and $\Delta\xi = \Delta\eta = \Delta x = \Delta y$ = 7.4 μm. Substituting these values into Eq. (7), the minimum object distance, $d \geq$ 140.17 mm, is obtained.

B. Correlation Coefficient Method

The CC between images measures the degree to which two images are similar. The value of the CC approaches 0 if there is no similarity between images and 1 if there is perfect similarity. The CC is defined as

$$\mathrm{CC} = \left[\frac{\sum_m\sum_n (F_{mn}-\overline{F})(G_{mn}-\overline{G})}{\sqrt{\left[\sum_m\sum_n (F_{mn}-\overline{F})^2\left[\sum_m\sum_n (G_{mn}-\overline{G})^2\right]\right]}}\right], \quad (8)$$

where m and n are the pixel indices, F and G are the images, and $\overline{F}$ and $\overline{G}$ are the mean gray levels of F and G. Figure 3 shows schematically how to determine the focal plane of particles by using CCs. A series of images are reconstructed slice by slice with the reconstruction interval, Δz. The CC at an arbitrary plane along the optical axis is evaluated by using two images at the same distance as half of the correlation interval, $\Delta C_z/2$, from that plane.

To calculate the intensity distribution of reconstruction images along the z axis, the numerical simulation of particle holograms was conducted based on

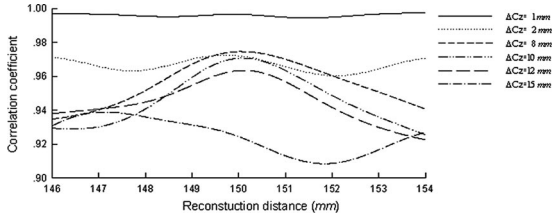

Fig. 7. Effect of correlation interval on the CC (object distance, d = 150 mm).

Eq. (5). After reconstructing many holograms with different particle sizes and object distances, the intensity distribution curves of reconstruction images were found to have a similar symmetrical shape, as shown in Fig. 4. Based on this kind of curve, the intensity of two symmetrical images at each side of the focal plane should be the same, and thus, the value of the CC at the focal plane should be maximum. The focal plane can be determined by choosing the peak point from the CC curve.

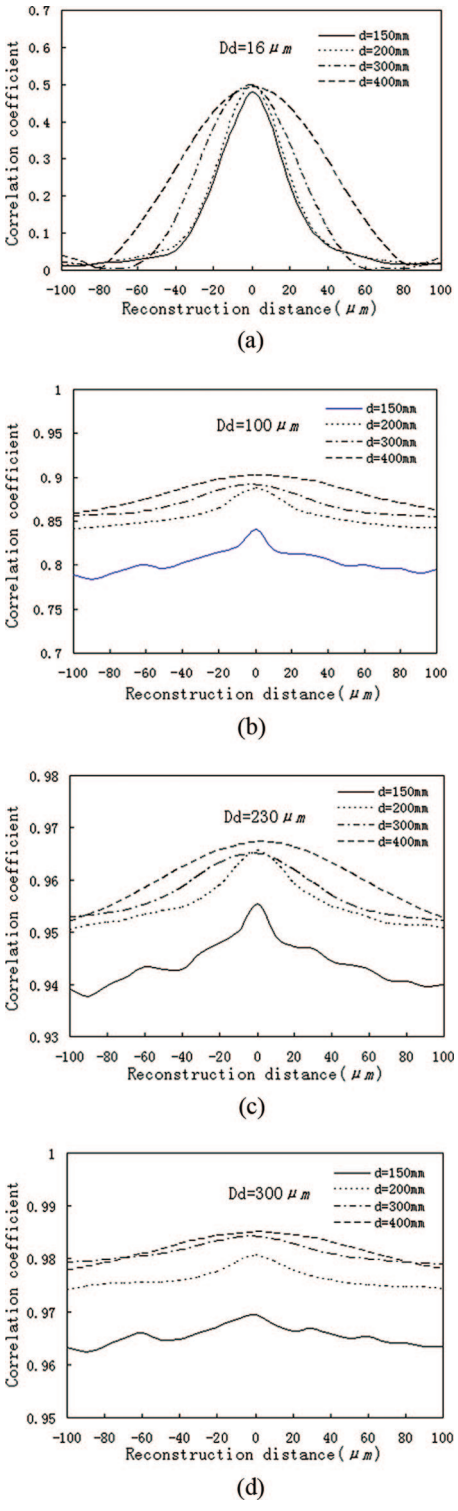

Fig. 8. (Color online) Effect of particle size and object distance on the CC: (a) $D_d = 16$ μm, (b) $D_d = 100$ μm, (c) $D_d = 230$ μm, (d) $D_d = 300$ μm.

Table 1. Errors of Focal Plane Determination by CC Method[a]

Size, D_d (μm)	Object Distance, d (mm)										
	150	160	170	180	200	210	220	230	240	300	400
16	10	0	0	0	0	0	0	0	0	−20	10
100	0	−10	0	0	0	−10	5	15	10	−20	30
300	0	0	0	0	0	0	0	−20	15	−30	30
500	−10	5	10	0	5	−10	10	20	20	−30	25

[a]Unit: micrometers.

As shown in Fig. 5, for the results of the focal plane determination of different sized particles in optical holography, the CC method can only be used for large particles ($D_d > 50$ μm), because the peaks produced by small particles cannot be distinguishable from those by noises and speckles. In optical holography, there are no effective ways to exclude this kind of noise at the hologram recording stage on holographic films. The reconstruction image recorded by a CCD camera can only be processed. So, there are a lot of noises in particle images reconstructed by optical holography, which can be confused as small sized particles. Whereas in digital holography, a majority of noises existing both in holograms recorded by a CCD camera and in particle images reconstructed numerically can be easily removed by using adequate filters. The quality of the reconstruction image of digital holography is better than that of optical holography. In this paper, the CC method is applied to digital particle holography to determine the focal plane of various sized particles, including much smaller sized particles ($D_d \sim 10$ μm).

3. Focal Plane Determination in Numerical Simulation Holograms

A. Using the Correlation Coefficient Method

The optimal values of the parameters in the CC method are also determined by the numerical simulation of particle holograms such as those used in Section 2. For the reconstruction interval, Δz, the number of reconstruction images is inversely propor-

Table 2. Errors of Focal Plane Determination by Gradient Method[a]

Size, D_d (μm)	Object Distance, d (mm)										
	150	160	170	180	200	210	220	230	240	300	400
16	40	20	90	−20	50	20	10	20	90	10	−10
100	40	80	−70	20	−30	0	70	100	−70	25	90
300	10	70	20	20	90	−80	−90	−90	90	50	90
500	20	−20	20	70	10	10	10	80	30	80	80

[a]Unit: micrometers.

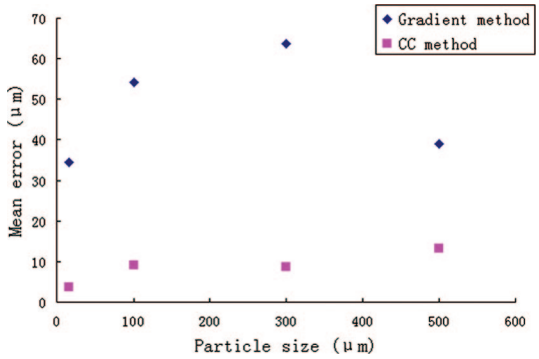

Fig. 9. (Color online) Comparison of errors for the CC and gradient methods.

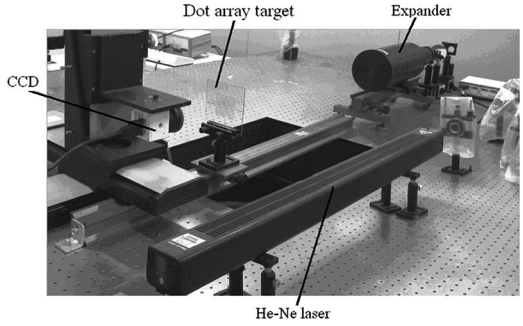

Fig. 11. Experimental setup of in-line digital holography.

tional to the value of Δz. For small Δz, the precision can be increased, but the calculation time is also increased greatly. For example, when we applied the CC method to a particle hologram to locate the focal plane (the pixel number, N, was 2048, and the calculation distance was 5 mm with Intel Core 2–2.4 GHz CPU), the calculation time was almost 10 h using $\Delta z = 1$ μm, whereas it was 1 h using $\Delta z = 10$ μm. In this paper, considering the measurement accuracy and efficiency of calculation, the reconstruction interval, Δz, was chosen as 10 μm. At this reconstruction interval, the error, which is defined as the difference between the object distance and the predicted focal plane, can be expressed as $e = \pm n \times \Delta z/2 = \pm n \times 5$ μm, $n = 0, 1, 2, \ldots$. The half of Δz is introduced because the focal plane is located in the middle of two image planes when the CC curve has two consecutive peaks. From the viewpoint of application to particle measurements, the level of error <20 μm is fully acceptable for our purpose. If higher accuracy is required, the reconstruction interval can be reduced with the sacrifice of a much longer calculation time.

For the optimal correlation interval, ΔC_z, the difference in the CC values at z_4 and z_7 positions in Fig. 3 should be big enough to easily obtain the peak. The difference in the CC values at z_4 and z_7 positions with the change of the correlation interval is shown in Fig. 6, which was obtained by the numerical simulation of holograms with a $D_d = 75$ μm particle. At the correlation interval of 10 mm, the difference in the CC values at z_4 and z_7 positions is the biggest. The distribution of CCs with several correlation intervals is also shown in Fig. 7. At too large or too small correlation intervals, the focal plane cannot be determined accurately. Based on the above results, the optimal value of the correlation interval was chosen as $\Delta C_z = 10$ mm. At this interval, the curve looks more symmetrical, and the peak point considered as the focal point exactly agrees with the corresponding object distance.

After determination of the optimal correlation interval, the effects of the particle size, D_d, and the object distance, d, were investigated, as shown in Fig. 8. The value of CCs is directly proportional to the object distance and particle size. Regardless of the various particle sizes and object distances, the peak of the curve indicating the focal plane can be easily determined. The error is defined as the difference between the predicted focal plane and the real object distance. The errors at different particle sizes and object distances are shown in Table 1. The errors for the object distance between $d = 150$ mm and $d = 220$ mm are within acceptable range, but the errors for the objects located over $d = 220$ mm are large. Based on this result, and the condition of Fresnel approximation derived by Eq. (7), the interval of the optimal object distance can be between $d = 150$ mm and $d = 220$ mm.

B. Using the Gradient Method

In the focal plane determination, a conventional solution is the gradient method [2,10], which is based on the sharpness of the object, i.e., the intensity gradient of the particle image. The sharpness is defined as the normalized sum of absolute numerical gradient values, calculated at the particle border. We applied this conventional method to the same simu-

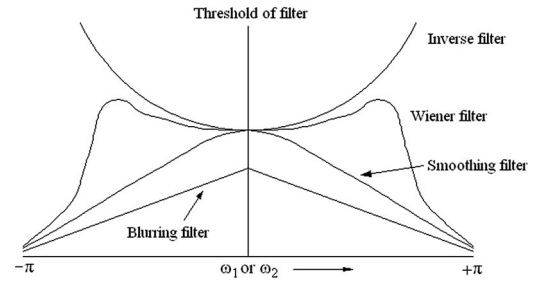

Fig. 10. Characteristics of self-adaptive Wiener filter.

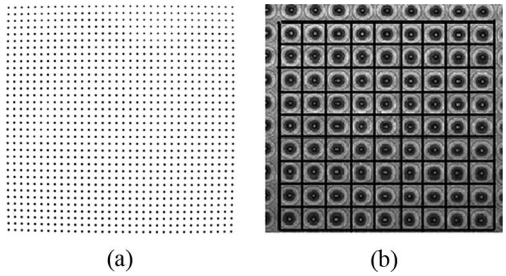

Fig. 12. Dot array target and its hologram: (a) dot array target and (b) hologram of local target showing ROIs of 81 dots.

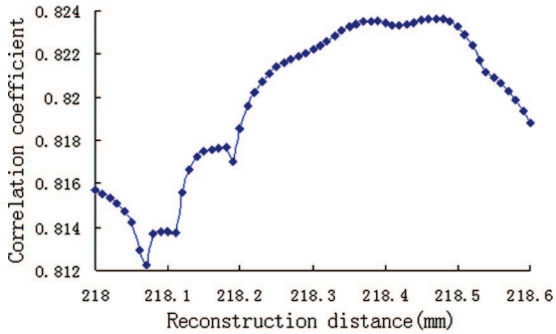

(a)

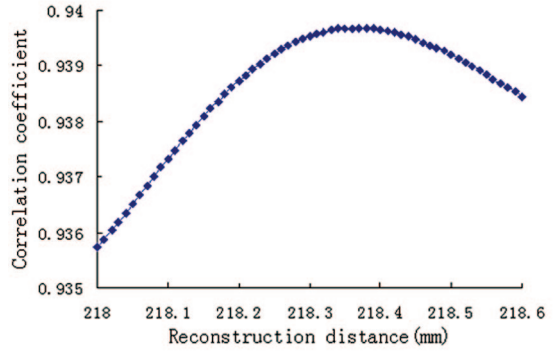

(b)

Fig. 13. (Color online) Application of Wiener filter: (a) without filtering and (b) with filtering.

lation holograms used for the CC method to compare the accuracy of both methods.

Using the gradient method for the focal plane of particles in simulation holograms, the errors of various particle sizes at different object distances are shown in Table 2. All errors are much bigger than those of the CC method except for a few points. The average of errors for each particle size obtained by two methods is compared in Fig. 9. The results clearly show that the CC method is superior to the classical gradient technique and has higher accuracy.

4. Application to Real Digital Holograms

A. Noise Removal

The CC method is applied to real digital holograms by using the optimal parameters discussed before. Actual digital holograms contain many inherent noises due to various experimental conditions and components. Therefore, an image processing technique to eliminate these noises is introduced first. To remove

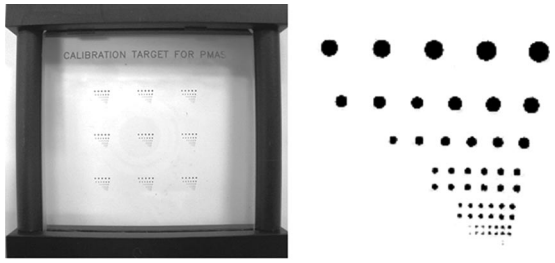

(a) (b)

Fig. 14. Calibration target with different sized particles: (a) calibration target and (b) magnified images of different sized dots.

noises in holographic images, adequate filtering methods were examined: the inverse filter [11], the subtraction method [12], the Gaussian high-pass filter, and the spectral filter [13]. Among various filters considered, we adopted the self-adaptive Wiener filter [14] for the preprocessing of digital holograms and postprocessing of reconstruction images. The self-adaptive Wiener filter executes an optimal trade-off between inverse filtering and noise smoothing. It tailors itself to be the "best possible filter" for a given data set by removing the additive noise and inverting the blurring, simultaneously. The Wiener filter in Fourier domain can be expressed as [14]

$$G(\omega_1,\ \omega_2) = \frac{H^*(\omega_1,\ \omega_2)S_{uu}(\omega_1,\ \omega_2)}{|H(\omega_1,\ \omega_2)|^2 S_{uu}(\omega_1,\ \omega_2) + S_{\eta\eta}(\omega_1,\ \omega_2)}, \tag{9}$$

where $S_{uu}(\omega_1, \omega_2)$ and $S_{\eta\eta}(\omega_1, \omega_2)$ are the power spectra of the original image and the noise, respectively, $H^*(\omega_1, \omega_2)$ is the inverse filter, and $H(\omega_1, \omega_2)$ is the blurring filter. It is easy to see that the Wiener filter has two separate parts, an inverse filtering part and a noise smoothing part. It not only performs the deconvolution by inverse filtering ($S_{\eta\eta} = 0$, high-pass filtering) but also removes the noise with a compression operation ($H = 1$, low-pass filtering). Figure 10 shows the characteristics of the Wiener filter. The Wiener filter uses the neighborhoods of fixed size to estimate the local image mean and standard deviation. In the present paper, we used the pixelwise adaptive method based on statistics estimated from a local neighborhood of each pixel in the MATLAB software.

Using the experimental setup, which is shown in Fig. 11, we recorded the in-line digital hologram of the dot array target to verify the feasibility of the

Table 3. Effect of Wiener Filter on Errors of Focal Plane Determination

Object Distance, z (mm)		Mean of Focal Planes (mm)	Mean of Errors (μm)	Standard Deviation of Errors (μm)
155.799	Without filtering	155.824	10.790	7.375
	With filtering	155.799	4.235	4.080
185.234	Without filtering	185.159	23.074	11.584
	With filtering	185.234	17.103	11.465

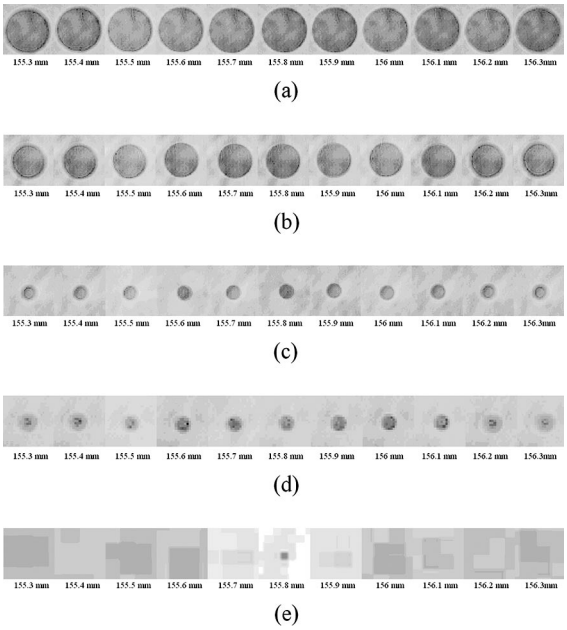

Fig. 15. Reconstruction images of particles at different reconstruction distances: (a) D_d = 300 μm; (b) D_d = 230 μm; (c) D_d = 100 μm; (d) D_d = 51 μm [the scale is two times of (c)]; (e) D_d = 10 μm [the scale is five times of (c)].

Wiener filter in the CC method for focal plane determination. The wavelength of the He–Ne laser is 0.6328 μm, the pixel size of the CCD is 7.4 μm, and the pixel number is 2048. The dot array target and its hologram showing regions of interest (ROIs) of 81 dots are shown in Fig. 12. The area of each ROI is ~2.25 mm^2 (210 × 210 pixels), and the area ratio of particle to ROI is 8.75%. The application of the Wiener filter to an arbitrary dot is shown in Fig. 13. The Wiener filter can be used to produce a much better shape of the CC curve, from which the focal plane can be easily determined.

After image processing of noisy holograms and reconstruction images, the focal planes of each particle are obtained using the CC method. The mean value of the focal planes is assumed as the optimal focal plane of the target, which can be the real position of the target from the CCD camera. The error is defined as the difference between the predicted focal plane of each dot and the mean value of the focal planes. The effect of the Wiener filter is shown in Table 3 at two different object distances. The Wiener filter greatly reduced the error of the focal plane, which proves that

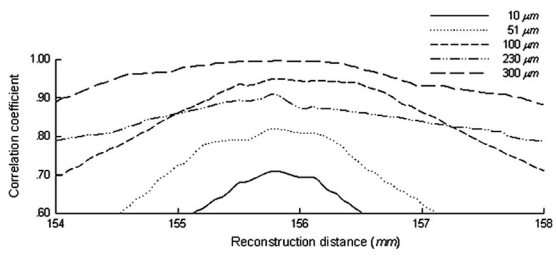

Fig. 16. Variation of the CC for different dot sizes.

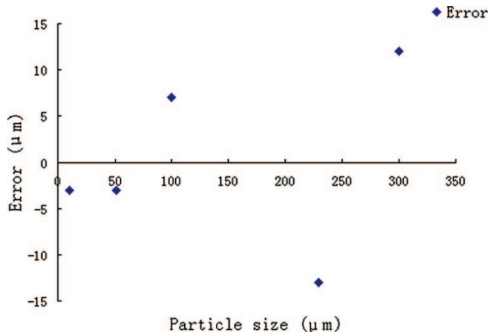

Fig. 17. (Color online) Errors of the focal plane for different dot sizes.

the filter has an excellent ability to reduce noise in holograms or reconstruction images. The mean value of the focal planes of each dot with application of the Wiener filter is considered as the actual position of the target. The results in Table 3 also show that the error of the focal plane is increased with the increase of the object distance; this trend was discussed before by simulation of holograms.

B. Different Dot Size

Using the same experimental setup and the calibration target (shown in Fig. 14), which has various dot sizes ranging from 8 to 300 μm, we investigated the variation of the CC method with the change of dot size. The position of the calibration target, which is the mean value of the focal planes of each dot, is 155.799 mm. The area ratio of particle to ROI is maintained the same as that of the dot array target. The reconstruction images of particles with different sizes at different depths are shown in Fig. 15. It shows that the depth of focus is proportional to the particle size. Figure 16 shows the CCs at different dot sizes of 10, 51, 100, 230, and 300 μm. The results are consistent with those discussed in the numerical simulation of holograms. As the size of the particles increases, the CC curve becomes flat, but regardless of particle size, the CC method can locate the focal plane without any difficulty.

The errors of the focal plane for different dot sizes are shown in Fig. 17. As already discussed in the simulation of holograms, the errors are proportional to the particle size, but all errors exist within an acceptable range of tolerance regardless of dot sizes. The mean of errors is 7.6 μm, and the standard deviation of errors is 4.271 μm.

In our experiments, simple 2D dots were used to simulate 3D particles. However, the holographic images produced by dots in 2D are similar to those generated by 3D particles such as opaque solid spheres or transparent liquid droplets, because the particle image is produced mainly by the entire or partial blocking of light. Even though the shape of the CC curve may change in 3D particles, we can still obtain the peak as the focal plane of objects. Therefore, the current results can be applicable to 3D particles.

5. Conclusions

We applied the CC method for determination of the focal plane to in-line digital particle holography. It is based on the theory of image comparability in which two symmetrical images at each side of the focal plane should be most similar. This method is first verified in the numerical simulation of holograms. The factors that influence this method, such as the correlation interval and the object size and distance, were examined, and then the optimal values of the correlation interval and the object distance interval were obtained. The particle size had no noticeable influence on the results of the CC method. For real digital holograms, the Wiener filter was introduced to remove noise in the digital holograms and the reconstruction images. Using the dot array target, the Wiener filter was proved to be an effective tool for removing noise and improving the position accuracy in the determination of the focal plane. Finally, the CC method was applied to the calibration target, which had dots of various sizes, and the results showed that the method produced errors within an acceptable range of tolerance regardless of dot sizes. Based on all these findings, the CC method can be an effective tool for determination of the focal plane in digital particle holography.

References

1. U. Schnars and W. Jueptner, "Digital recording and numerical reconstruction of holograms," Meas. Sci. Technol. **13,** 85–101 (2002).
2. L. Yu and L. Cai, "Iterative algorithm with a constraint condition for numerical reconstruction of a three-dimensional object from its hologram," J. Opt. Soc. Am. A **18,** 1033–1045 (2001).
3. F. Dubois, C. Schockaert, N. Callens, and C. Yourassowsky, "Focus plane detection criteria in digital holography microscopy by amplitude analysis," Opt. Express. **14,** 5895–5980 (2006).
4. C. B. Lefebvre, S. Coëtmellec, D. Lebrun, and C. Özkul, "Application of wavelet transform to hologram analysis: three-dimensional location of particles," Opt. Lasers Eng. **33,** 409–421 (2000).
5. Y. Zhang, D. X. Zheng, J. L. Shen, and C. L. Zhang, "3D locations of the object directly from in-line holograms using the Gabor transform," Proc. SPIE **5636,** 116–120 (2005).
6. Y. J. Choo and B. S. Kang, "The characteristics of the particle position along an optical axis in particle holography," Meas. Sci. Technol. **17,** 761–770 (2006).
7. U. Schnars and W. Jueptner, "Digital holography," in *Digital Holography: Digital Hologram Recording, Numerical Reconstruction, and Related Techniques* (Springer, 2005), pp. 41–45.
8. Y. Yang and B. S. Kang, "Numerical simulation of in-line digital holograms," in *Proceedings of Asia Display 2007,* H. S. Kwok, ed. (East China Normal U. Press, 2007), pp. 2055–2059.
9. J. W. Goodman, "Fresnel and Fraunhofer diffraction," in *Introduction to Fourier Optics,* 3rd ed. (Roberts & Company, 2005), pp. 68–72.
10. V. Ilchenko, T. Lex, and T. Sattelmayer, "Depth position detection of the particles in digital holographic particle image velocimetry (DHPIV)," Proc. SPIE **5851,** 123–128 (2005).
11. L. Denis, C. Fournier, T. Fournel, and C. Ducottet, "Twin-image noise reduction by phase retrieval in in-line digital holography," Proc. SPIE **5914,** 148–161 (2005).
12. V. R. Singh and A. K. Asundi, "Amplitude contrast image enhancement in digital holography for particles analysis," Proc. SPIE **5878,** 17.1–17.8 (2005).
13. S. Kim and S. J. Lee, "Effect of particle concentration on digital holographic PTV measurement," J. Korea Soc. Mech. Eng. B **30,** 929–934 (2006).
14. A. K. Jain, "Image filtering and restoration," in *Fundamentals of Digital Image Processing,* T. Kailath, ed. (Prentice-Hall, 1989), pp. 276–306.